Analytica Chimica Acta 1056 (2019) 153–160

Contents lists available at ScienceDirect

Analytica Chimica Acta

journal homepage: www.elsevier.com/locate/aca

Label-free fluorometric assay for cytochrome c in apoptotic cells based on near infrared Ag_2S quantum dots

Meifang Cai, Caiping Ding, Xuanyu Cao, Fangfang Wang, Cuiling Zhang*, Yuezhong Xian**

Shanghai Key Laboratory of Green Chemistry and Chemical Processes, Department of Chemistry, School of Chemistry and Molecular Engineering, East China Normal University, Shanghai, 200241, China

HIGHLIGHTS

- A simple, label-free approach was developed to detect Cyt c using near infrared fluorescence Ag_2S QDs.
- The sensing strategy is based on the peroxidase-like activity of the hydrolysate of Cyt c.
- The Ag_2S QDs – based strategy is due to electron transfer mechanism.
- The strategy was successfully applied for the measurement of Cyt c in the apoptotic cells inducing by H_2O_2 or etoposide.

GRAPHICAL ABSTRACT

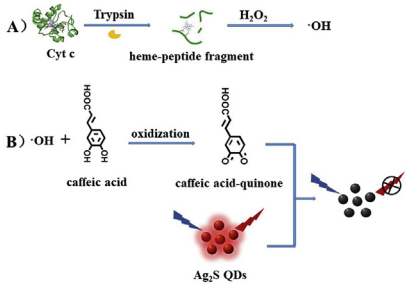

ARTICLE INFO

Article history:
Received 17 October 2018
Received in revised form
16 December 2018
Accepted 5 January 2019
Available online 8 January 2019

Keywords:
Near infrared
Quantum dots
Biosensor
Cyt c
Anticancer drug

ABSTRACT

As an important biomarker, cytochrome c (Cyt c) plays a crucial role in mitochondrial electron transport chain and cell apoptosis. Herein, a label-free near-infrared (NIR) Ag_2S quantum dots (QDs)-based fluorescent strategy was constructed for the sensitive and selective detection of Cyt c. In this system, Cyt c was hydrolyzed by trypsin, and the resulting heme-peptide fragment exhibited peroxidase-like activity for catalytic decomposition of H_2O_2 into hydroxyl radical (·OH). The presence of caffeic acid in this system resulted into the formation of caffeic acid-quinone due to the strong oxidizing ability of ·OH. The production of caffeic acid-quinone led to the fluorescence quenching of Ag_2S QDs through electron transfer mechanism. Based on the cascade reaction, we successfully developed a label-free approach to detect Cyt c using Ag_2S QDs as nanoprobes. Under the optimized conditions, the fluorescence intensity of Ag_2S QDs was linearly relative to the concentration of Cyt c over the range from 2.0 to 150 nM with a detection limit of 1.7 nM. In addition, this strategy was successfully applied for quantitative detection of Cyt c in cell lysates of H_2O_2 or etoposide (anticancer drug)-induced apoptotic cells, providing great potential application for cell-based oxidation pressure determination and screening of anticancer drugs.

1. Introduction

Cytochrome c (Cyt c), a heme-containing protein, plays a critical physiological role in the cell apoptosis process [1]. Normally, Cyt c exists in mitochondrial membrane in cells and can be acted as an electron carrier due to its iron content. Once Cyt c releases from mitochondria and enters into cytoplasm, it can trigger the

* Corresponding author.
** Corresponding author.
E-mail addresses: clzhang@chem.ecnu.edu.cn (C. Zhang), yzxian@chem.ecnu.edu.cn (Y. Xian).

https://doi.org/10.1016/j.aca.2019.01.005
0003-2670/

activation of caspases and stimulate apoptosis [2,3]. Thus, Cyt c has been considered to be an indicator of the apoptotic process in the cell [4–6]. Therefore, the detection of Cyt c in cell lysates is of important significance to learn about certain diseases on cellular level [7,8]. On account of the facts, it is crucial to develop novel strategies for sensitive and selective detection of Cyt c.

Until now, various methods have been reported for detecting Cyt c, such as enzyme linked immunosorbent assay (ELISA) [9], flow cytometry [10], HPLC [11], electrophoresis [12] and electrochemical method [13]. The signal amplification in ELISA is mediated by enzymatic reaction, which is limited by the availability of substrates [14]. As for flow cytometry, HPLC and electrophoresis, these approaches possess sufficient sensitivity, but with the shortages of time-consuming and expensive instruments [14,15]. Electrochemical method is easy to be interfered by electrochemical active substances and the electrode surface is prone to be passivated by the proteins [14–16]. Recently, an electrochemiluminescence aptasensor was developed for the detection of Cyt c, which was based on the immobilization of negatively charged apatmer on reduced graphene oxide (rGO)/$Ru(bpy)_3^{2+}$–CeO_2 nanoparticle-chitosan [17]. An optical microfiber aptasensor with a Ag@rGO nanointerface was reported for real-time cellular Cyt c monitoring, which was based on the change of surface refractive index induced by the surface roughness and thickness resulted from the capturing Cyt c [18]. Fluorescence assay has been extensively applied in biological analysis due to its simple operation, high sensitivity and low cost [19,20]. Recently, the nanoprobes based on fluorophore-tagged aptamer were constructed for the detection of Cyt c [21–23]. Based on the adsorption and fluorescence quenching abilities, VS_2 nanosheet-based fluorescent biosensor was developed for the selective and sensitive detection of Cyt c using fluorescein-labeled aptamer as recognizer and probes [14]. Shamsipur and coworkers developed an aptamer-templated Ag nanoclusters for the selective and sensitive detection of Cyt c based on the photoinduced electron transfer mechanism. The fluorescent probe was successfully employed for the detection of early stage of apoptosis based on the measurement of Cyt c released from the mitochondria of HEK293T cells, which were treated with CCLR buffer and anticancer drug Doxorubicin [15]. An upconvertion@polydopamine (UCNP@PDA) core@shell nanoparticle-based fluorescence activated aptameric biosensor was also developed for the ratiometric detection of Cyt c, in which Cy3 modified aptamer was used to recognize Cyt c, and UCNP@PDA NP was acted as an internal reference and fluorescence quenching agent [21]. Very recently, Yang's group reported an azoreductase and Cyt c double activated fluorescent aptameric sensor for specific distinguishing of the release of Cyt c in apoptotic process induced by hypoxia [23]. Although the aptameric fluorescence biosensors show highly selective for Cyt c detection, the screening and labelling are tedious and expensive. The integration of fluorescent nanomaterials with molecular imprinting technique is another choice for selective detection of Cyt c through the combination of molecular imprinting technique with UCNPs [24], nitrogen-doped-graphene quantum dots (GQDs)@SiO_2, [25] and Si QDs@ SiO_2 [26]. However, for the protein imprinting, this procedure is very difficult to be realized and the reproducibility of this strategy is not easy to be controlled. The label-free strategy with high sensitivity and selectivity is urgently needed for the measurement of Cyt c. The interaction between Cyt c and thioglycolic acid (TGA) modified CdTe QDs resulted into the fluorescence quenching due to the enhancement of electron transfer via the coordination of TGA sulfur with Cyt c iron. The system was developed to be a bioanalytical platform for Cyt c detection in human SKIN cells and bioimaging in primary human dermal fibroblasts [27]. Through the integration of GQDs with GO, Cao developed a fluorescent sensing platform for recognition of Cyt c by modulation the fluorescence signal "turn-on" or "turn-off" via different interaction model with Cyt c [28]. [Poly(styrene-4-sulfonate)-protected copper nanoclusters were also developed to detect Cyt c based on the quenching effect of Cyt c [29]. Although label-free fluorescence methods were also developed for detection of Cyt c based on carbon QDs [30], CdTe QDs [27], gold and silver nanoclusters [15], graphene QDs [28], etc, however, most of these nanomaterials emit visible fluorescence. The autofluorescent from proteins under the excitation of UV–vis light might affect the accurate analysis of the early stage apoptotic cells through the detection of Cyt c released from mitochondrial. Near-infrared (NIR) fluorescence is a very promising tool for biosensing due to minimal autofluorescence, absorption of biomolecules and light scattering. Therefore, there are still high demands to develop a simple, label-free NIR fluorescent method for detection of Cyt c in biological samples.

Since Wang and coworkers reported to synthesize NIR Ag_2S QDs [31], the nanomaterials have attracted intensive attention for biomedical applications. Due to the absence of toxic metal ions and ultralow solubility product constant ($K_{sp} = 6.3 \times 10^{-50}$), Ag_2S QDs show excellent biocompatibility [32]. Moreover, Ag_2S QDs have been widely applied in biosensing and bioimaging due to their unique properties, including excellent NIR emitting, unusual photochemical stability and high penetration depth [33]. Herein, a simple and label-free method was developed for Cyt c detection by using NIR Ag_2S QDs as the sensing probe in this work. As shown in Scheme 1, Cyt c is hydrolyzed into heme-peptide fragments by trypsin, and the hydrolysis products with peroxidase-like activity can convert H_2O_2 into ·OH. Then, the released ·OH can oxidize caffeic acid to form caffeic acid-quinone [34–36], and lead to the fluorescence quenching of Ag_2S QDs via electron transfer [37–40]. Hence, the presence of Cyt c in sensing system can trigger the cascade reaction and turn off the fluorescence of Ag_2S QDs. The approach has been successfully applied in detection of Cyt c in cell lysates, which is released from apoptotic cells induced by H_2O_2 and anticancer drug etoposide.

2. Experimental section

2.1. Materials and chemicals

Cyt c, caffeic acid, trypsin, 3,3′,5,5′-tetra-methylbenzidine (TMB), etoposide, ascorbic acid, lysozyme and lysine were acquired from Aladdin Industrial Co., Ltd (Shanghai, China). Hemin, IgG, Hb and transferrin were obtained from Sigma-Aldrich (Shanghai, China). 3-mercaptopropionic acid (3-MPA, 99%) was purchased from J&K Chemical Technology Co., Ltd (Shanghai, China). Glutathione (GSH), H_2O_2, $AgNO_3$ and NaOH were obtained from Sinopharm Chemical Reagent Co., Ltd (Shanghai, China). Albumin from bovine serum (BSA), adenosine triphosphate (ATP) and tris(hydroxymethyl)aminomethane (Tris) were purchased from Sangon Biotech Co., Ltd. (Shanghai, China). Dulbecco's modified Eagle's Medium (DMEM), penicillin-streptomycin and trypsin solution were obtained from Sangon Biotechnology Co., Ltd. (Shanghai, China). Ultrapure water (18.2 MΩ cm) was used in all the experiments.

2.2. Apparatus

Fluorescence spectra and lifetime were measured by a FLS 980 fluorescence spectrometer (Edinburgh Instruments Ltd, UK). UV–vis spectra were recorded by a UV-2550 spectrophotometer (Shimadzu, Japan). Fourier transform infrared (FTIR) spectra were obtained at room temperature on a Thermo Scientific Nicolet iS50 FTIR spectrometer. Transmission electron microscopy (TEM) imaging was obtained by a JEM-2100F TEM (JEOM, Japan). X-ray

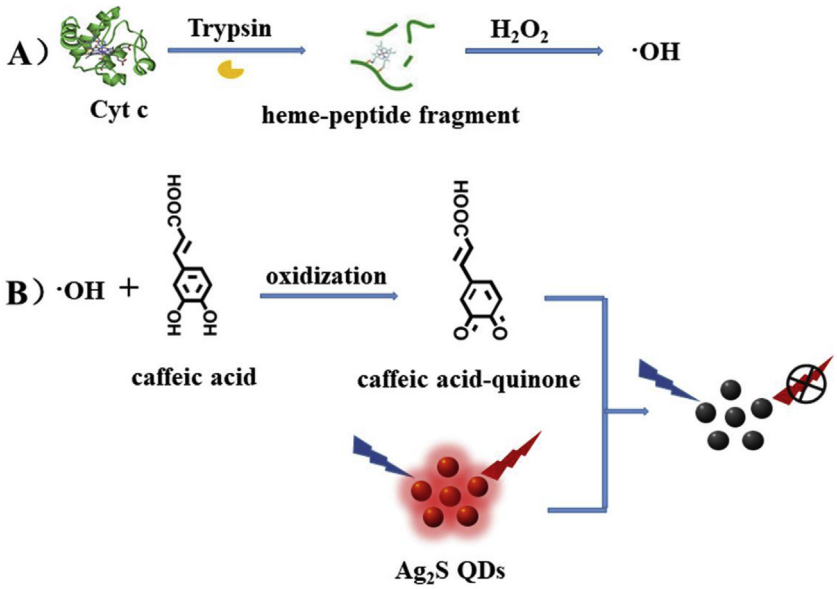

Scheme 1. Schematic illustration of the label-free detection of Cyt c based on NIR Ag_2S QDs.

powder diffraction (XRD) pattern was conducted by a D8 Advance X-ray powder diffractometer (Bruker, Germany). The X-ray photoelectron spectra (XPS) were measured by an AXIS Ultra DLD X-ray photoelectron spectrometer (Shimadzu, Japan).

2.3. Synthesis of Ag_2S QDs

Water-dispersible Ag_2S QDs were synthesized according to previous work of our group [41]. Generally, 25 mM 3-MPA mixed with 45 ml deionized water under nitrogen for 30min.Then, 5 mM $AgNO_3$ was added, and the pH was adjusted to around 7.5 using NaOH and CH_3COOH solutions (2 mol L^{-1}). The solution was heated to 90 °C under magnetic stirring for 12 h. The resulted product was washed with ultrapure water using centrifugal filtration devices (Molecular weight cutoff or MWCO 3 kDa, Millipore Amico Ultra) and then stored at 4 °C for further usage. The concentration of QDs in colloidal solution was measured by inductively coupled plasma optical emission spectrometer (ICP-OES).

2.4. Peroxidase-like activity of heme-peptide fragment

0.2 μM Cyt c and 5 μg/ml trypsin were reacted for 60 min at 37 °C in acetic acid buffer (50 mM, pH = 5.0). Then, 0.5 mM TMB and 200 μM H_2O_2 were quickly added into above solution and the UV–vis absorption spectra were measured within 2 min.

2.5. Fluorescent detection of Cyt c

Different concentrations of Cyt c and 5 μg/ml trypsin were dissolved in Tris-HCl buffer (50 mM, pH = 8.0) at 37 °C for 60 min 100 μM caffeic acid, 200 μM H_2O_2 and 30 μL Ag_2S QDs (0.5 mg/ml) were added, subsequently. After incubating 60 min at room temperature, the fluorescence intensities of the above solutions were recorded on FLS 980 fluorescence spectrometer (λ_{ex} = 468 nm).

2.6. Cell culture and induction of apoptosis

Hela cells were grown in DMEM (high glucose) and replenished with 1% penicillin-streptomycin and 10% FBS (fetal bovine serum) at 37 °C and 5% CO_2. In order to induce the cell apoptosis, 50 μM H_2O_2 or 5 μM etoposide was added and incubated with Hela cells (1×10^5 cells) for 12 h, respectively. Then, the cultured Hela cells were washed four times with PBS, and then trypsinized, pelleted by centrifugation (1000 rpm for 3 min). The supernatant was removed and resuspended in 200 μL PBS. After that, the resuspended cells solution was frozen at −20 °C for 30 min and thawed at 37 °C for 5 min. The frozen and thawed processes were repeated three times, and the cell lysate was centrifuged at 12000 rpm for 1 min at 4 °C. The supernatant was stored in refrigerator at 4 °C for further usage.

2.7. Detection of Cyt C in cell lysates

Cyt c in cell lysates collected from above experimental process was detected by using standard addition method. 10 μL cell lysates and various amounts of Cyt c were added, and the following procedures were the same as the fluorescence detection.

3. Results and discussion

3.1. Characterization of Ag_2S QDs

The morphology of Ag_2S QDs was characterized by TEM (Fig. 1A). The as-synthesized Ag_2S QDs show good dispersibility and the average particle size is about 3.57 ± 0.02 nm (based on the statistics of 350 QDs) (Fig. 1B). XRD was used to investigate the crystal structure of Ag_2S QDs. The experimental data indicate the Ag_2S QDs with monoclinic pattern (JCPDS Card No. 65–2356) (Fig. 1C). The broadening of the diffraction peaks may be attributed to the nature of nanocrystalline and amorphous surface ligands [31,42,43]. FITR spectra of 3-MPA and Ag_2S QDs are shown in Fig. 1D. As for 3-MPA, the absorption peak located at 2574 cm^{-1} is corresponding to the stretch vibration of free thiol group. The band at 1713 cm^{-1} is attributed to the C=O stretch vibration of carboxyl group. As for Ag_2S QDs, the peak at 2574 cm^{-1} almost disappears, indicating that 3-MPA is successfully bound to the surface of Ag_2S QDs via the Ag-thiol interaction. The strong signals at 1562 and 1416 cm^{-1} are assigned to the asymmetric and symmetric stretching vibration of carboxylate [44]. The XPS analysis confirmed the chemical composition of the as-prepared QDs. Fig. S1 shows the Ag 3d and S

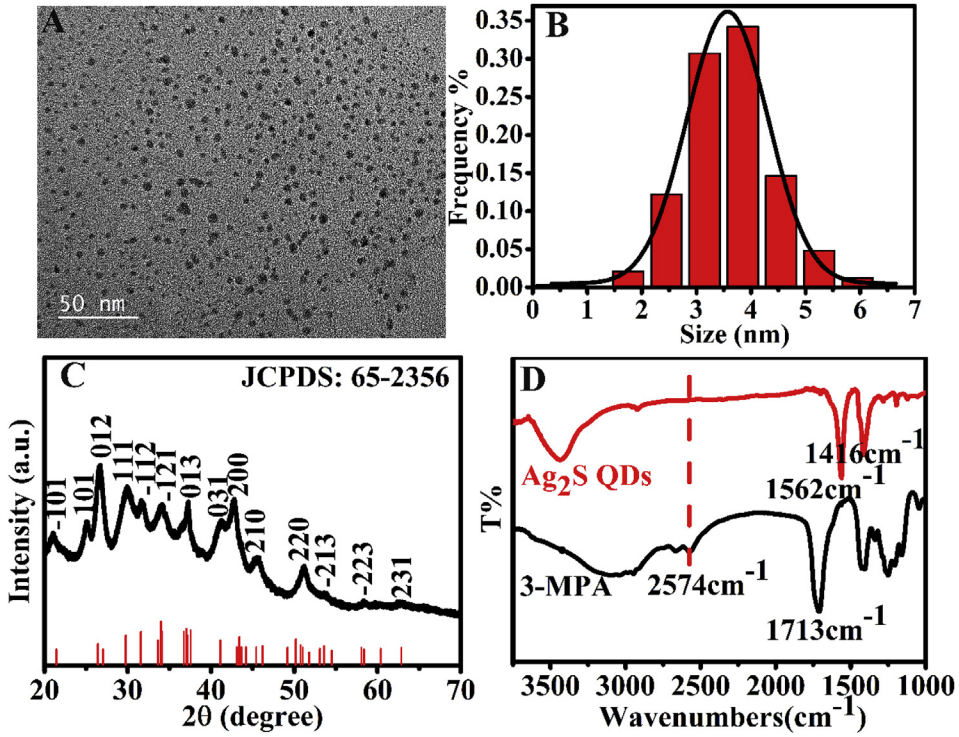

Fig. 1. (A) TEM image and (B) the corresponding size distribution of Ag_2S QDs, (C) Powder XRD pattern of Ag_2S QDs (the line in the bottom is the standard XRD pattern of monoclinic Ag_2S crystals (JCPDS no. 65–2356)), (D) FTIR spectra of Ag_2S QDs (red curve) and 3-MPA (black curve). (For interpretation of the references to colour in this figure legend, the reader is referred to the Web version of this article.)

2p core level peaks of Ag_2S QDs. The binding energies (BE) of the Ag $3d_{5/2}$ and $3d_{3/2}$ appear at 368.25 and 374.27 eV, indicating the existence of the oxidation state of Ag (I) in the Ag_2S QDs (Fig. S1A) [43]. The S 2p core level could be fitted to two doublet sets (Fig. S1B). The S $2p_{3/2}$ peak at 162.18 eV is indicative of an Ag–S–Ag bond originating from the inorganic core and the peak at 163.39 eV belongs to S of the 3-MPA [44]. All data show that 3-MPA is conjugated on the surface of Ag_2S QDs. We further investigated the optical properties of the as-prepared Ag_2S QDs. As shown in Fig. S2 (black line), no obvious absorption peak is observed, in contrast, Fig. S2 (red and blue line) shows that Ag_2S QDs display strong luminescence at 790 nm with the excitation wavelength of 468 nm. The results are consistent with literature [41].

3.2. Principles of the sensing system

To explore the peroxidase-like activity of heme-peptide fragment, the classic reaction of H_2O_2-mediated TMB oxidization was adopted (Fig. S3). There are no obvious characteristic absorption peaks for oxidized TMB at 652 nm in the systems of TMB (Fig. S3(a)), TMB/H_2O_2 (Fig. S3(b)) and TMB/H_2O_2/trypsin (Fig. S3(c)). After addition of Cyt c into TMB/H_2O_2/trypsin system, a strong absorption for oxidized TMB is observed (Fig. S3(e)). However, for the TMB/H_2O_2/Cyt c system, only a very weak absorption is observed (Fig. S3(d)). These data show that the peroxidase-like activity is resulted from the hydrolysate of Cyt c, namely, heme-peptide fragment [45].

To confirm the caffeic acid can be oxidized into caffeic acid-quinone during the process, we investigated the UV–vis spectra of caffeic acid before and after adding into the Cyt c/trypsin/H_2O_2 system (Fig. 2A). As shown in Fig. 2A (a) and (d), broad absorption peak at 420–550 nm appears in the presence of Cyt c, trypsin and H_2O_2. It is the characteristic absorption of quinonoid species [46], indicating the formation of caffeic acid-quinone [18,36,47,48]. The system coexistence of Cyt c, trypsin and H_2O_2 can produce ·OH with strong oxidizing ability and result into the oxidation of caffeic acid and formation of caffeic acid-quinone [34,49–51]. Based on the UV–vis spectra for other controlled systems, they are further confirmed the absorption at 420–550 nm is due to the formation of caffeic acid-quinone. Fig. 2A (b) and (c) are the UV–vis spectra for caffeic acid/H_2O_2 and caffeic acid/Cyt c/trypsin systems, respectively. It can be seen that no obvious absorption appears at 420–550 nm. Fig. 2B (a) is the UV–Vis spectrum of Cyt c, and the characteristic absorption for γ (Sorbet) band (at 410 nm), β band (at 522 nm), and α band (at 550 nm) can be observed. All data indicate that the Cyt c is in a reduced state [52,53]. In the presence of trypsin, the absorption at 410 nm is blue-shifted to 405 nm, the peaks at 522 nm and 550 nm are lost and a small broad band appears. These changes suggest that the Cyt c is hydrolyzed to form heme-peptide fragment, the heme cofactor in heme-peptide fragment is exposed to the external environment and which can be oxidized quickly [54,55]. These results indicate that caffeic acid is oxidized into caffeic acid-quinone by ·OH produced during the process.

The fluorescence intensities of Ag_2S QDs were further investigated in different system. As shown in Fig. 2C(a-e), the fluorescence intensities of Ag_2S QDs remain stable, indicating these substances, such as caffeic acid, trypsin, H_2O_2 or their reaction products, do not affect the luminescence emission of Ag_2S QDs. Based on the observation on Fig. 2B(c) and (e), we can draw a conclusion that Cyt c and its hydrolysate also cannot change the fluorescent features of Ag_2S QDs. Moreover, the fluorescence intensity of Ag_2S QDs remains stable in the system of H_2O_2 and caffeic acid, indicating that caffeic acid cannot be oxidized by H_2O_2 to yield caffeic acid-quinone. Only in the system of Cyt c/caffeic acid/trypsin/H_2O_2, the fluorescence spectrum of Ag_2S QDs is obviously changed. In this

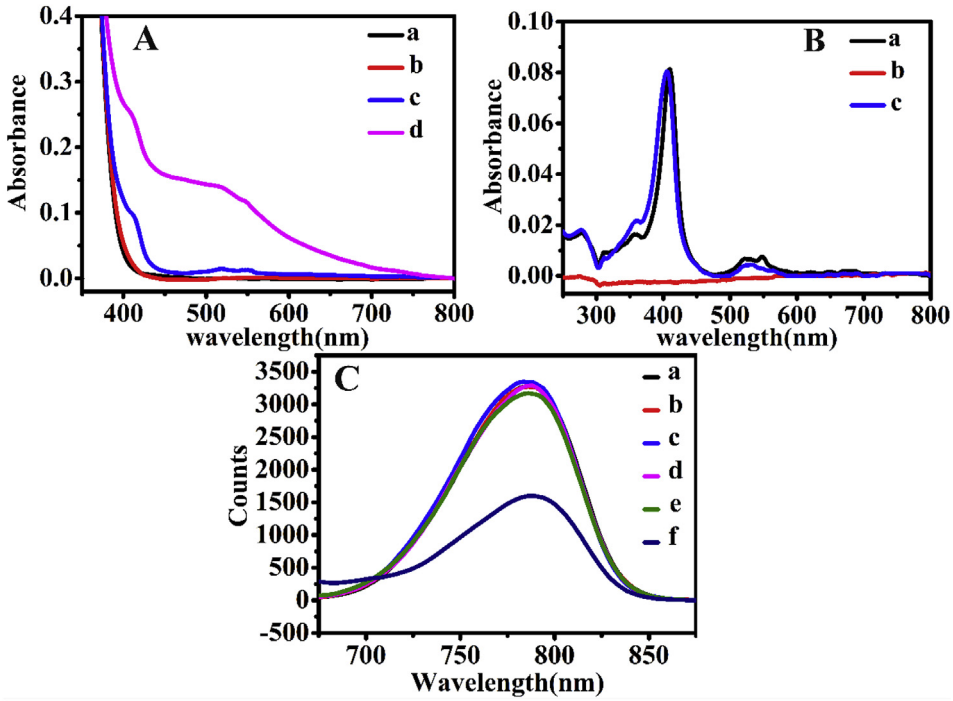

Fig. 2. (A) UV–vis absorption spectra of (a) caffeic acid, (b) caffeic acid/H_2O_2, (c) caffeic acid/Cyt c/trypsin, (d)caffeic acid/Cyt c/trypsin/H_2O_2; (B) UV–vis absorption spectra of (a) Cyt c, (b) trypsin, (c) Cyt c/trypsin; (C) Fluorescence spectra of Ag_2S QDs (a) and in presence of trypsin/caffeic acid/H_2O_2 (b), Cyt c (c), caffeic acid/H_2O_2 (d), Cyt c/trypsin (e), Cyt c/trypsin/caffeic acid/H_2O_2 (f).

system, the presence of Cyt c induces significant fluorescence quenching of Ag_2S QDs due to the formation of caffeic acid-quinone through cascade reaction. Based on these facts, Cyt c can be detected through the changes of fluorescent intensity of Ag_2S QDs.

The quenching mechanism is further investigated in detail. Based on above-mentioned experiments, the fluorescence of Ag_2S QDs was quenched by the formation of caffeic acid-quinone. It was reported that quinones were efficient quenchers for fluorescent nanomaterials, such as QDs and noble metal nanoclusters via electron transfer mechanism [37–40]. As electron shuttles, quinones can accept the electrons and deliver them from the conduction band to valence band [40]. Therefore, we believed that the fluorescence quenching of Ag_2S QDs by caffeic acid-quinone is also through electron transfer. In order to verify the mechanism, the fluorescence lifetime of Ag_2S QDs in buffer and in the system of Cyt c/caffeic acid/trypsin/H_2O_2 was measured and further fitted with a two-exponential decay function (Fig. 3). The average fluorescence lifetime of Ag_2S QDs (Fig. 3a) is 18.4 ns with lifetime components of 10.34 ns (29.32%) and 21.79 ns (70.68%). In the system of Cyt c/caffeic acid/trypsin/H_2O_2 system (Fig. 3b), the average fluorescence lifetime is decreased to 10.5 ns with lifetime components of 5.56 ns (33.55%) and 12.93 ns (66.45%). The significant changes in fluorescence lifetime indicate the dynamic quenching process, which is consistent with electron transfer mechanism. Although the Förster resonance energy transfer (FRET) could affect the fluorescence lifetime, it is lack of any spectral overlap between the emission spectrum of Ag_2S QDs and absorption spectrum of Cyt c/caffeic acid/trypsin/H_2O_2 system (Fig. S2(red line), Fig. 2A(d)). Therefore, the FRET process is ruled out and electron transfer is the predominate mechanism for Cyt c detection.

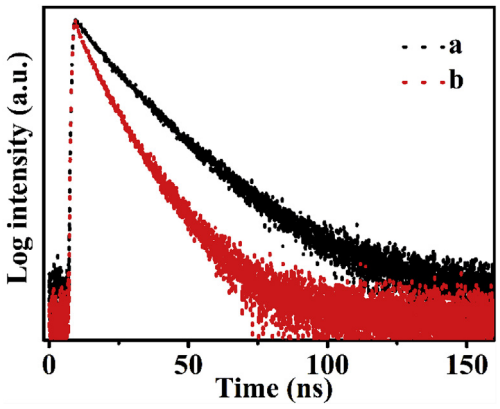

Fig. 3. Fluorescence lifetimes of Ag_2S QDs in the absence (a) and presence of Cyt c/trypsin/caffeic acid/H_2O_2 (b).

3.3. Detection of Cyt c

To get the best performance of the fluorescence assay, the experimental conditions were optimized. Firstly, the effect of solution pH on the signal of Ag_2S QDs was evaluated in the range from 1 to 12 (Fig. S4A). The maximum fluorescence intensity is obtained around pH 8. Then, the effect of ionic strength was also investigated. It is found that the fluorescence intensities of Ag_2S QDs remain stable while the ionic strength was varied from 0 to 250 mM at pH 8 (Fig. S4B). At last, the time-dependent change of fluorescence from Ag_2S QDs in the system of Cyt c/trypsin/caffeic acid/H_2O_2 was exhibited in Fig. S4C. It can be seen that the fluorescence intensity of Ag_2S QDs decreases rapidly within 20 min and remains almost constant after 60 min. Thus, 60 min was selected as the optimum incubation time.

Under optimal conditions, the performance of the method was tested. Various concentrations of Cyt c were added into the system of trypsin/caffeic acid/H_2O_2/Ag_2S QDs. With the increase of the amounts of Cyt c from 2.0 nM to 0.2 μM, the fluorescence intensities

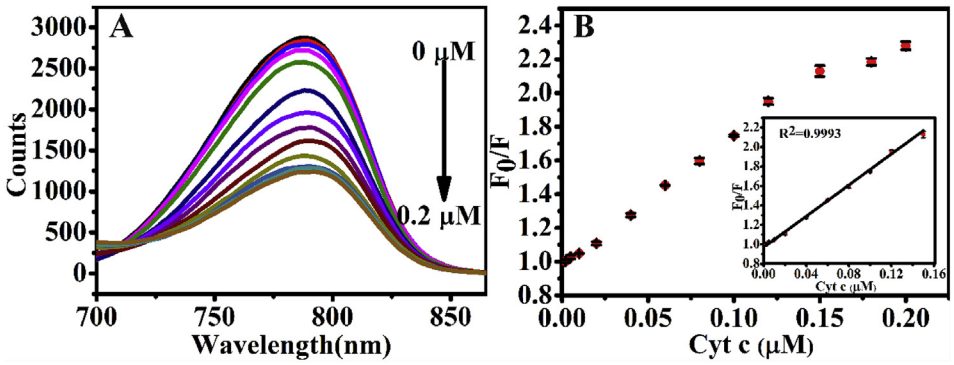

Fig. 4. (A) Fluorescence spectra of Ag_2S QDs in the system of trypsin/caffeic acid/H_2O_2/with Cyt c (0, 0.002, 0.005, 0.01, 0.02, 0.04, 0.06, 0.08, 0.10, 0.12, 0.15, 0.18, 0.2 μM). (B) The fluorescence intensity ratio F_0/F against Cyt c concentration (0.002–0.2 μM). F_0 and F are the fluorescence intensities of Ag_2S QDs in the absence and presence of Cyt c, respectively. The inset in Fig. 4B is the linear response for Cyt c assay.

Table 1
Comparison of the performance of different fluorescent methods for Cyt c detection.

Nanomaterials	Fluorescence system and signal	Liner range	Detection limit	Ref.
aptamer/AgNCs	label-free; 610 nm	0–1.0 μM	15.7 nM	[15]
CdTe QDs	label-free; 550 nm	0.5–2.5 μM	500 nM	[27]
molecularly imprinted UCNP	label; 543.5 nm	1–24 μM	730 nM	[24]
carbon QDs	label-free; 455 nm	1–30 μM	0.3 nM	[30]
UCNPs@polydopamine	label; 570 nm	0.05–10 μM	20 nM	[21]
Graphene oxide/fluorophore-tagged DNA aptamer	label; 664 nm	0.03–10 μM	10 nM	[56]
AuNPs/fluorophore-tagged DNA aptamer	label; 580 nm	0.1–10 μM	16.7 nM	[23]
graphitic carbon nitride nanosheets	label-free; 450 nm	16–140 nM	2.6 nM	[16]
Ag_2S ODs	label-free; 790 nm	2–150 nM	1.7 nM	This work

decreased gradually (Fig. 4A). As shown in Fig. 4B, the fluorescence intensity ratio F_0/F exhibits an excellent linear relationship with the concentration of Cyt c ($R^2 = 0.9993$) over the range of 2.0 nM to 0.15 μM, and the limit of detection is about 1.7 nM (based on 3 s/m). Compare with other fluorescence methods, the performance of our assay is comparable (Table 1). Moreover, our fluorescent technique is also superior when compare with other different detection techniques, which are listed in Table S1.

To verify the applicability of the assay in cell lysates for Cyt c, the specificity of the sensing system was tested. The fluorescence responses to other proteins (i.e., Lyz, transferrin, IgG, BSA and Hb) as well as small biomolecules (ATP, GSH, Lys and hemin) were evaluated, and the results are shown in Fig. 5. Compare with Cyt c, the influences of other substances on the fluorescence intensity can be

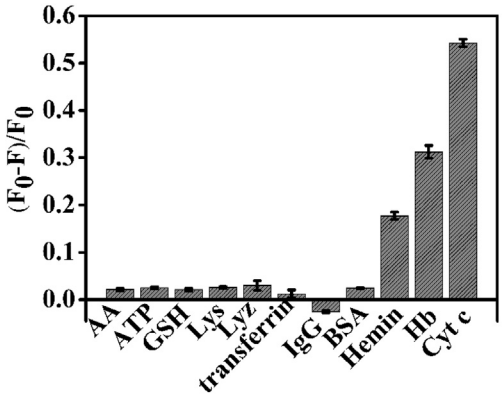

Fig. 5. The selectivity of the system for Cyt c detection. The concentrations of AA, ATP, GSH, Lys, Lyz, transferrin, IgG, BSA, Hemin and Hb are the same as Cyt c (0.2 μM). F_0 and F are the fluorescence intensities of the sensing system in the absence and presence of interfering substances respectively.

ignored except for Hb and hemin. it arises from the Hb and hemin also contain the heme group, the Hb also can be hydrolyzed by trypsin, the hydrolysate also can catalyze H_2O_2 to produce ·OH to some extent and oxidize caffeic acid to caffeic acid-quinone, thus Hb and hemin can affect the fluorescence intensity of Ag_2S QDs. Meanwhile, it is worth noting that Cyt c, Hb and hemin have different origins [15]. Hb is presented in the red blood cells, and Cyt c exists in inner membrane of the mitochondria. Moreover, in the cell lysate, Hb or hemin does not exist in the presence of Cyt c, and vice versa [15]. Therefore, those interfering substances cannot affect the detection of Cyt c in cell lysates.

3.4. Detection Cyt c released from apoptotic cells

Taking advantages of high specificity and sensitivity, the fluorometric assay was employed for label-free detection of Cyt c released from apoptotic cells. In this procedure, H_2O_2 and etoposide were utilized to induce cells apoptosis, respectively. Standard addition method was used to evaluate the reliability of our method, and the results are summarized in Table 2. As one of the most

Table 2
Detection of Cyt c released from Hela cells treated with H_2O_2 and etoposide, respectively.

Treated by	Spiked (nM)	Found (nM)	Recovery (n = 3) (%)
H_2O_2 (50 μM)	0	17.2 ± 0.2	
	10	27.6 ± 0.4	104.0 ± 4.5
	50	68.1 ± 0.2	101.8 ± 0.6
	100	115.3 ± 0.8	98.1 ± 0.8
Etoposide (5 μM)	0	24.5 ± 0.4	
	10	34.0 ± 0.5	95.0 ± 6.4
	50	74.0 ± 0.3	99.0 ± 1.0
	100	126.6 ± 0.4	102.1 ± 0.6

important ROS, high concentration level H_2O_2 in cells can generate oxidative pressure and lead to apoptosis [57]. Etoposide, as an anticancer drug, can also induce the apoptosis of cells. Table 2 shows the data of detection of Cyt c in HeLa cells induced by H_2O_2 and etoposide, respectively. The results are comparable with other methods [21,58]. Moreover, the quantitative detection of Cyt c is achieved with an acceptable recovery of 95.0–104.0%. It is worth to note that our method shows the potential abilities for anticancer drug screening and oxidative stress monitoring.

4. Conclusions

We constructed a simple, label-free method for Cyt c detection based on NIR Ag_2S QDs. In this work, we developed a cascade reaction to yield the fluorescent quencher, which was triggered by Cyt c. The heme-peptide fragment with peroxidase-like activity was produced from Cyt c hydrolyzed by trypsin, and catalyzes H_2O_2 to release ·OH. In the presence of caffeic acid, it was oxidized by ·OH to yield caffeic acid-quinone and resulted into the fluorescence quenching of Ag_2S QDs via electron transfer mechanism. The assay shows selective and sensitive detection for Cyt c with a very low limit in the nanomolar level. Due to the minimal autofluorescence, absorption of biomolecules and light scattering of near infrared fluorescence, this strategy has been successfully applied in measurement of Cyt c in the apoptotic cells induced by H_2O_2 or etoposide. It means the method may offer an opportunity for anticancer drug screening and oxidation pressure determination. In a word, our developed strategy not only offers a simple, label free and NIR fluorescent method for Cyt c detection, but also broadens the application of Ag_2S QDs in biological analysis.

Declaration of interests

The authors declare that they have no known competing financial interests or personal relationships that could have appeared to influence the work reported in this paper.

Acknowledgements

This work was financially supported from National Key R&D Program of China (2018YFF0215404), National Natural Science Foundation of China (21605050, 11727810), Shanghai Natural Science Foundation (18ZR1411300), and the Postdoctoral Science Foundation of China (2018T110367).

Appendix A. Supplementary data

Supplementary data to this article can be found online at https://doi.org/10.1016/j.aca.2019.01.005.

References

[1] M. Hüttemanna, P. Pecina, M. Rainbolt, T.H. Sanderson, V.E. Kagan, L. Samavatia, J.W. Doan, I. Lee, The multiple functions of cytochrome c and their regulation in life and death decisions of the mammalian cell: from respiration to apoptosis, Mitochondrion 11 (2011) 369–381.
[2] E.B. Wetzel, D.D. Newmeyer, D.R. Green, Mitochondrial cytochrome c release in apoptosis occurs upstream of DEVD-specific caspase activation and independently of mitochondrial transmembrane depolarization, EMBO J. 17 (1998), 37-491998.
[3] M.O. Hengartner, The biochemistry of apoptosis, Nature 407 (2000) 770–776.
[4] X. Liu, C.N. Kim, J. Yang, R. Jemmerson, X. Wang, Induction of apoptotic program in cell-free extracts: requirement for dATP and cytochrome c, Cell 86 (1996) 147–157.
[5] S. Zhang, S. Zhu, L. Yang, Y. Zheng, M. Gao, S. Wang, J.Z. Zeng, X. Yan, High-throughput multiparameter analysis of individual mitochondria, Anal. Chem. 84 (2012) 6421–6428.
[6] J.M. Song, P.M. Kasili, G.D. Griffin, T. Vo-Dinh, Detection of cytochrome c in a single cell using an optical nanobiosensor, Anal. Chem. 76 (2004) 2591–2594.
[7] M. Cao, C. Cao, M. Liu, P. Wang, C. Zhu, Selective fluorometry of cytochrome c using glutathione-capped CdTe quantum dots in weakly basic medium, Microchim. Acta. 165 (2009) 341–346.
[8] Y. Shen, X.-F. Yang, Y. Wu, C. Li, Sensitive spectrofluorimetric determination of cytochrome c with spirocyclic rhodamine B hydrazide in micellar medium, J. Fluoresc. 18 (2008) 163–168.
[9] J.M. Song, P.M. Kasili, G.D. Griffin, T. Vo-Dinh, Detection of cytochrome c in a single cell using an optical nanobiosensor, Anal. Chem. 76 (2004) 2591–2594.
[10] C.B. Campos, B.A. Paim, R.G. Cosso, R.F. Castilho, H. Rottenberg, A.E. Vercesi, Method for monitoring of mitochondrial cytochrome c release during cell death: immunodetection of cytochrome c by flow cytometry after selective permeabilization of the plasma membrane, Cytometry 69 (2006) 515–523.
[11] E.D. Crouser, M.E. Gadd, M.W. Julian, J.E. Huff, K.M. Broekemeier, K.A. Robbins, D.R. Pfeiffer, Quantitation of cytochrome c release from rat liver mitochondria, Anal. Biochem. 317 (2003) 67–75.
[12] S.N. Tan, L. Hua, Amperometric detection of cytochrome c by capillary electrophoresis at a sol–gel carbon composite electrode, Anal. Chim. Acta 450 (2001) 263–267.
[13] X.W. Hu, C.J. Mao, J.M. Song, H.L. Niu, S.Y. Zhang, H.P. Huang, Fabrication of GO/PANi/CdSe nanocomposites for sensitive electrochemiluminescence biosensor, Biosens. Bioelectron. 41 (2013) 372–378.
[14] X. Yin, J. Cai, H. Feng, Z. Wu, J. Zou, Q. Cai, A novel VS_2 nanosheet-based biosensor for rapid fluorescence detection of cytochrome c, New J. Chem. 39 (2015) 1892–1898.
[15] M. Shamsipur, F. Molaabasi, S. Hosseinkhani, F. Rahmati, Detection of early stage apoptotic cells based on label-free cytochrome c assay using bioconjugated metal nanoclusters as fluorescent probes, Anal. Chem. 88 (2016) 2188–2197.
[16] F. Salehnia, M. Hosseini, M.R. Ganjali, A fluorometric aptamer based assay for cytochrome C using fluorescent graphitic carbon nitride nanosheets, Microchim. Acta 184 (2017) 2157–2163.
[17] M.R.K. Pur, M. Hosseini, F. Faridbod, M. Reza Ganjali, S. Hosseinkhani, Early detection of cell apoptosis by a cytochrome C label-Free electrochemiluminescence aptasensor, Sensor. Actuator. B Chem. 257 (2018) 87–95.
[18] H. Li, Y. Huang, C. Chen, A. Xiao, G. Hou, Y. Huang, X. Feng, B. Guan, Real-Time cellular cytochrome C monitoring through an optical microfiber: enabled by a silver-decorated graphene nanointerface, Adv. Sci. 5 (2018), 1701074.
[19] Y.J. Gong, X.B. Zhang, G.J. Mao, L. Su, H.M. Meng, W.H. Tan, S.L. Feng, G.S. Zhang, A unique approach toward near-infrared fluorescent probes for bioimaging with remarkably enhanced contrast, Chem. Sci. 7 (2016) 2275–2285.
[20] A.Q. Zhang, C.M. Lieber, Nano-bioelectronics. Chem. Rev. 116 (2016) 215–257.
[21] L. Ma, F. Liu, Z. Lei, Z. Wang, A novel upconversion@ polydopamine core@ shell nanoparticle based aptameric biosensor for biosensing and imaging of cytochrome c inside living cells, Biosens. Bioelectron. 87 (2017) 638–645.
[22] T. Chen, X. Tian, C. Liu, J. Ge, X. Chu, Y. Li, Fluorescence activation imaging of cytochrome c released from mitochondria using aptameric nanosensor, J. Am. Chem. Soc. 137 (2015) 982–989.
[23] J. Tang, C. Huang, J. Shu, J. Zheng, D. Ma, J. Li, R. Yang, Azoreductase and target simultaneously activated fluorescent monitoring for cytochrome c release under hypoxia, Anal. Chem. 90 (2018) 5865–5872.
[24] T. Guo, Q. Deng, G. Fang, C. Liu, X. Huang, S. Wang, Molecularly imprinted upconversion nanoparticles for highly selective and sensitive sensing of Cytochrome c, Biosens. Bioelectron. 74 (2015) 498–503.
[25] Y. Yan, X. He, W. Lia, Y. Zhang, Nitrogen-doped graphene quantum dots-labeled epitope imprinted polymer with double templates via the metal chelation for specific recognition of cytochrome c, Biosens. Bioelectron. 91 (2017) 253–261.
[26] X. Zhang, Y. Qin, H. Ye, X. Ma, X. He, W. Li, Y. Zhang, Silicon nanoparticles coated with an epitope-imprinted polymer for fluorometric determination of cytochrome c, Microchim. Acta 185 (2018) 173.
[27] R.M. Amin, S.A. Elfeky, T. Verwanger, B. Krammer, Fluorescence-based CdTe nanosensor for sensitive detection of cytochrome C, Biosens. Bioelectron. 98 (2017) 415–420.
[28] L. Cao, X. Li, L. Qin, S. Kang, G. Li, Graphene quantum dots supported by graphene oxide as a sensitive fluorescence nanosensor for cytochrome c detection and intracellular imaging, J. Mater. Chem. B 5 (2017) 6300–6306.
[29] Y. Hu, Y. He, Y. Han, Y. Ge, G. Song, J. Zhou, Poly (styrene-4-sulfonate)-protected copper nanoclusters as a fluorometric probe for sequential detection of cytochrome c and trypsin, Microchim. Acta 185 (2018) 383.
[30] H. Zhang, B. Zhang, C. Di, M.C. Ali, J. Chen, Z. Li, J. Si, H. Zhang, H. Qiu, Label-free fluorescence imaging of cytochrome c in living systems and anti-cancer drug screening with nitrogen doped carbon quantum dots, Nanoscale 10 (2018) 5342–5349.
[31] Y. Du, B. Xu, T. Fu, M. Cai, F. Li, Y. Zhang, Q. Wang, Near-infrared photoluminescent Ag_2S quantum dots from a single source precursor, J. Am. Chem. Soc. 132 (2010) 1470–1471.
[32] R. Gui, A. Wan, X. Liu, W. Yuan, H. Jin, Water-soluble multidentate polymers compactly coating Ag_2S quantum dots with minimized hydrodynamic size and bright emission tunable from red to second near-infrared region, Nanoscale 6 (2014) 5467–5473.
[33] H. Jin, R. Gui, J. Gong, W. Huang, Aptamer and 5-fluorouracil dual-loading Ag2S quantum dots used as a sensitive label-free probe for near-infrared photoluminescence turn-on detection of CA125 antigen, Biosens. Bioelectron. 92 (2017) 378–384.

[34] P. Xu, H. Uyama, J.E. Whitten, S. Kobayashi, D.L. Kaplan, Peroxidase-catalyzed in situ polymerization of surface orientated caffeic acid, J. Am. Chem. Soc. 127 (2005) 11745–11753.
[35] F. Kader, M. Irmouli, J.P. Nicolas, M. Metche, Proposed mechanism for the degradation of pelargonidin 3-glucoside by caffeic acid o-quinone, Food Chem. 75 (2001) 139–144.
[36] N. Cai, Y. Li, S. Chen, X. Su, A fluorometric assay platform for caffeic acid detection based on the G-quadruplex/hemin DNAzyme, Analyst 141 (2016) 4456–4462.
[37] J. Yuan, W. Guo, E. Wang, Utilizing a CdTe quantum dots–enzyme hybrid system for the determination of both phenolic compounds and hydrogen peroxide, Anal. Chem. 80 (2008) 1141–1145.
[38] I.L. Medintz, M.H. Stewart, S.A. Trammell, K. Susumu, J.B. Delehanty, B.C. Mei, J.S. Melinger, J.B. Blanco-Canosa, P.E. Dawson, H. Mattoussi, Quantum-dot/dopamine bioconjugates function as redox coupled assemblies for in vitro and intracellular pH sensing, Nat. Mater. 9 (2010) 676–684.
[39] R. Gill, R. Freeman, J. Xu, I. Willner, S. Winograd, I. Shweky, U. Banin, Probing biocatalytic transformations with CdSe– ZnS QDs, J. Am. Chem. Soc. 128 (2006) 15376–15377.
[40] C. Burda, T.C. Green, S. Link, M.A. El-Sayed, Electron shuttling across the interface of CdSe nanoparticles monitored by femtosecond laser spectroscopy, J. Phys. Chem. B 103 (1999) 1783–1788.
[41] C. Ding, X. Cao, C. Zhang, T. He, N. Hua, Y. Xian, Rare earth ions enhanced near infrared fluorescence of Ag_2S quantum dots for the detection of fluoride ions in living cells, Nanoscale 9 (2017) 14031–14038.
[42] P. Jiang, Z. Tian, C. Zhu, Z. Zhang, D. Pang, Emission-tunable near-infrared Ag_2S quantum dots, Chem. Mater. 24 (2012) 3–5.
[43] L. Tan, A. Wan, H. Li, Conjugating S-nitrosothiols with glutathiose stabilized silver sulfide quantum dots for controlled nitric oxide release and near-infrared fluorescence imaging, ACS Appl. Mater. Interfaces 5 (2013) 11163–11171.
[44] I. Hocaoglu, M.N.C. izmeciyan, R. Erdem, C. Ozen, A. Kurt, A. Sennaroglu, H.Y. Acar, Development of highly luminescent and cytocompatible near-IR-emitting aqueous Ag_2S quantum dots, J. Mater. Chem. 22 (2012) 14674–14681.
[45] L. Zhang, J. Du, A sensitive and label-free trypsin colorimetric sensor with cytochrome c as a substrate, Biosens. Bioelectron. 79 (2016) 347–352.
[46] M.I. Halawa, F. Wu, T.H. Fereja, B. Lou, G. Xu, One-pot green synthesis of supramolecular β-cyclodextrin functionalized gold nanoclusters and their application for highly selective and sensitive fluorescent detection of dopamine, Sensor. Actuator. B Chem. 254 (2018) 1017–1024.
[47] A. Rompel, H. Fischer, D. Meiwes, K.B. Karentzopoulos, A. Magrini, C. Eicken, C. Gerdemann, B. Krebs, Substrate specificity of catechol oxidase from Lycopus europaeus and characterization of the bioproducts of enzymic caffeic acid oxidation, FEBS Lett. 445 (1999) 103–110.
[48] C.Ž. Slavoljub, M.V. Aleksandar, Žarko J. Mitić, Goran M. Nikolić, The study of the influence of Mg(II) and Ca(II) ions on caffeic acid autoxidation in weakly alkaline aqueous solution using MCR-ALS analysis of spectrophotometric data, New J. Chem. 42 (2018) 6256–6263.
[49] S. Pati, I. Losito, F. Palmisano, P.G. Zambonin, Characterization of caffeic acid enzymatic oxidation by-products by liquid chromatography coupled to electrospray ionization tandem mass spectrometry, J. Chromatogr. A 1102 (2006) 184–192.
[50] J.L.J. Cilliers, V.L. Singleton, J. Agrie, Nonenzymic autoxidative phenolic browning reactions in a caffeic acid model system, Food Chem. 37 (1989) (1989) 890–896.
[51] M. Antolovich, D.R. Bedgood Jr., A.G. Bishop, D. Jardine, P.D. Prenzler, K. Robards, LC-MS investigation of oxidation products of phenolic antioxidants, J. Agric. Food Chem. 52 (2004) 962–971.
[52] A.A. Andrade, N.M. Barbosa Neto, L. Misoguti, L. De Boni, S.C. Zilio, C.R. Mendonca, Two-photon absorption investigation in reduced and oxidized cytochrome c solutions, Chem. Phys. Lett. 390 (2004) 506–510.
[53] H. Yue, Y. Kang, H. Zhang, X. Gao, R.E. Blankenship, Expression and characterization of the diheme cytochrome c subunit of the cytochrome bc complex in Heliobacterium modesticaldum, Arch. Biochem. Biophys. 517 (2012) 131–137.
[54] Q. Zhang, W. Li, J. Chen, F. Wang, Y. Wang, Y. Chen, C. Yu, An ultrasensitive chemiluminescence turn-on assay for protease and inhibitor screening with a natural substrate, Chem. Commun. 49 (2013) 3137.
[55] B.A. Springer, K.D. Egeberg, S.G. Sligar, R.J. Rohlfs, A.J. Mathews, J.S. Olson, Discrimination between oxygen and carbon monoxide and inhibition of autooxidation by myoglobin. Site-directed mutagenesis of the distal histidine, J. Biol. Chem. 264 (1989) 3057–3060.
[56] T. Chen, X. Tian, C. Li, W. Liu, J. Ge, X. Chu, Y. Li, Fluorescence activation imaging of cytochrome c released from mitochondria using aptameric nanosensor, J. Am. Chem. Soc. 137 (2015) 982–989.
[57] M. Ott, V. Gogvadze, S. Orrenius, B. Zhivotovsky, Mitochondria, oxidative stress and cell death, Apoptosis 12 (2007) 913–922.
[58] M. Pandiaraj, N.K. Sethy, K. Bhargava, V. Kameswararao, C. Karunakaran, Designing label-free electrochemical immunosensors for cytochrome c using nanocomposites functionalized screen printed electrodes, Biosens. Bioelectron. 54 (2014) 115–121.